Identification and analysis of microplastics in para-tumor and tumor of human prostate

Chenyao Deng,[a,d,e,f,g] Jun Zhu,[a,d,e,f,g] Zishui Fang,[a,d,e,f,g] Yuzhuo Yang,[b,g] Qiancheng Zhao,[a,d,e,f] Zhe Zhang,[c] Zirun Jin,[a,d,e,f,*] and Hui Jiang[a,d,e,f,**]

[a]Department of Urology, Peking University First Hospital, Beijing, 100034, China
[b]Department of Obstetrics and Gynecology, Peking University First Hospital, Beijing, 100034, China
[c]Department of Urology, Center for Reproductive Medicine, Peking University Third Hospital, Beijing, 100191, China
[d]The Institution of Urology, Peking University, Beijing, 100034, China
[e]Beijing Key Laboratory of Urogenital Diseases (Male) Molecular Diagnosis and Treatment Center, Beijing, 100034, China
[f]National Urological Cancer Center, Beijing, 100034, China

eBioMedicine
2024;108: 105360
Published Online xxx
https://doi.org/10.1016/j.ebiom.2024.105360

Summary

Background While microplastics are widely found in various human organs and tissues, the relationship between microplastics and human health, especially prostate health, remains unclear. This study aims to identify and quantify the properties, types, and abundance of microplastics in paired para-tumor and tumor tissues of human prostate. Additionally, the potential correlation between microplastics abundance and prostate cancer are investigated.

Methods Paired para-tumor and tumor samples of the prostate were collected from 22 patients who underwent robot-assisted radical prostatectomy. A combination of laser direct infrared spectroscopy, scanning electron microscopy and pyrolysis-gas chromatography-mass spectrometry was utilized to analyse the properties, type and abundance of microplastics. Correlations between microplastics abundance, demographic characteristics and clinical features of patients were also examined.

Findings Laser direct infrared analysis revealed the presence of microplastics, including polyamide, polyethylene terephthalate, and polyvinyl chloride, in both para-tumor and tumor tissues of human prostate. However, polystyrene was exclusively detected in tumor tissues. The particle size distribution in the prostate tissue mainly ranged from 20 to 100 μm. Approximately 31.58% of para-tumor samples exhibited sizes between 20 and 30 μm, while 35.21% of tumor samples displayed sizes between 50 and 100 μm. The shapes of these microplastics varied considerably with irregular forms being predominant. Additionally, microplastics were detected by pyrolysis–gas chromatography-mass spectrometry in 20 paired prostate tissues. The mean abundance of microplastics was found to be 181.0 μg/g and 290.3 μg/g in para-tumor and tumor of human prostate samples, respectively. Among the 11 target types microplastics polymers, only polystyrene, polypropylene, polyethylene, and polyvinyl chloride were detected. Notably, polystyrene, polyethylene, and polyvinyl chloride, except for polypropylene, demonstrated significantly higher abundance in tumor tissues compared to their respective paired para-tumor. Furthermore, a positive correlation was observed between polystyrene abundance in the tumor samples of human prostate and frequency of take-out food consumption.

Interpretation This research provides both qualitative and quantitative evidence of the microplastics presence as well as their properties, types, and abundance in paired para-tumor and tumor samples of human prostate. Correlations between microplastics abundance, demographics, and clinical characteristics of patients need to be further validated in future studies with a larger sample size.

Funding This work was supported by the National Key Research and Development Program of China (2022YFC2702600) and the National Natural Science Foundation of China (Grant No. 82071698, No. 82101676, and No. 82271630).

Keywords: Microplastics; Prostate cancer; Scanning electron microscopy; Laser direct infrared spectroscopy; Pyrolysis–gas chromatography-mass spectrometry

*Corresponding author. Department of Urology, Peking University First Hospital, Beijing, 100034, China.
**Corresponding author. Department of Urology, Peking University First Hospital, Beijing, 100034, China.
E-mail addresses: jinzirun@bjmu.edu.cn (Z. Jin), jianghui@bjmu.edu.cn (H. Jiang).
[g]These authors contributed equally to this work.

Research in context

Evidence before this study

Microplastics are ubiquitously distributed in virtually all human organs. A recent study has indicated that exposure to microplastics may time- and dose-dependently facilitate the proliferation of cutaneous squamous cell carcinoma cell line.[1] Our previous study also revealed the presence of microplastics in human semen and testis, suggesting their potential ability to traverse the blood-testis barrier. Numerous studies have addressed the impacts of microplastics on the digestive, respiratory, and endocrine systems of humans. While prostate is a vital organ within the urogenital system, its relationship with microplastics remains unclear.

Added value of this study

Here, we provided multiple lines of evidence demonstrating the existence of microplastics in both para-tumor and tumor tissues of human prostate. Through laser direct infrared spectroscopy, scanning electron microscopy, and pyrolysis-gas chromatography-mass spectrometry techniques, we have confirmed varying particle counts, sizes, shapes, types as well as concentrations of accumulated microplastics within these tissues. Furthermore, we preliminarily assessed possible correlations between microplastics abundance and demographic as well as clinical characteristics among these patients.

Implications of all the available evidence

According to our findings, microplastics can be found in both human prostate tumor and para-tumor tissues, but with differences in their abundance and type. The relationship between microplastics and prostate cancer needs to be further studied.

Introduction

Microplastics (MPs) are extensively utilized in various industries, including food, medicine, and agriculture. The widespread presence of MPs globally can be attributed to the population growth and industrial development witnessed in the 21st century.[2] Plastic production has surged by a staggering 230 times from 2 to 460 metric tons annually between 1950 and 2019, with a significant portion eventually transforming into microplastics.[3] Industrialized nations and regions such as North America, Europe, and East Asia serve as primary sources for plastics manufacturing and consumption due to substantial plastic waste generated by the plastics sector and consumer behaviour.[4,5] MPs constitute a crucial component of environmental pollution since plastic particles smaller than 5 mm in diameter are commonly found in soil, water, and air, thus they can easily enter the human body through the food chain.[6]

MPs have been detected within numerous human organs including placenta,[7] lungs,[8] intestines,[9] blood,[10] and even testes.[11] MPs also pose potential health risks for human beings owing to their strong affinity for hazardous compounds.[12] They may carry toxic plasticizers such as bisphenol A (BPA) and dibutyl phthalate (DBP).[13] Once absorbed into human bodies, MPs along with these adsorptive substances accumulate, resulting in detrimental effects on human health.[14]

Prostate cancer is one of the most common cancers among men worldwide. Its incidence increases with age and it encompasses several risk factors such as genetics, hormones, lifestyle and environmental pollution.[15,16] Change in level of androgen and increased inflammatory response caused by MPs exposure are closely associated with prostate cancer progression.[17–19] Similarly, BPA and Polycyclic Aromatic Hydrocarbons (PAH) can suppress gene expression, disturb the activity of androgen receptors and alter prostate cell morphology, eventually leading to oncogene expression.[20] However, it remains unclear whether there are different types and an abundance of MPs in the para-tumor and tumor tissues of human prostate. Additionally, the correlation between MPs and prostate cancer is still unknown.

In this study, we aimed to analyse and quantify the properties, types, and abundance of MPs in the para-tumor and tumor of prostate from 22 patients diagnosed with prostate cancer using laser direct infrared (LDIR) spectroscopy, scanning electron microscopy (SEM) and pyrolysis–gas chromatography-mass spectrometry (Py–GC/MS). Furthermore, we attempted to investigate the potential associations between MPs abundance, demographics, and clinical characteristics of prostate cancer patients.

Methods

Ethics statement

The present study was approved by the Ethics Committee of Peking University First Hospital (approved number: 2024–256) and was conducted according to the Declaration of Helsinki. All the participants have signed the informed consent form prior to robot-assisted radical prostatectomy (RARP).

Participants

Participants were patients who underwent RARP from January 2023 to July 2024 at Peking University First Hospital, thus, the recruitment response rate was 100%. Clinical data of 22 patients were collected. Inclusion criteria of participants were as following: 1) none of the patients had undergone neoadjuvant endocrine therapy before RARP; 2) preoperative examinations such as serum prostate specific antigen (PSA) value before

puncture, ultrasonic puncture biopsy, magnetic resonance scanning of the prostate and enhanced CT were perfect, and no distant metastases of prostate cancer were found; 3) RARP of all the patients were performed by senior doctors, and postoperative specimens were diagnosed as prostate cancer by at least 2 physicians in the Department of Pathology.

Samples collection

Para-tumor and tumor of the prostate were collected. Para-tumor tissues were identified as tissues which were at least 2 cm beyond the tumor tissue boundary. 22 paired para-tumor and tumor of the prostate (44 samples) were collected. Firstly, 2 paired tissues (4 samples) were used for LDIR and scanning electron microscopy analysis of MPs to initially verify the presence of MPs, then the other 20 paired tissues (40 samples) were used in Py-GC/MS to further quantify the MPs. To prevent the plastic pollution, we adhered to a strict plastic-free protocol throughout the sampling process. Cotton surgical gowns and polymer-free nitrile gloves were worn. Once obtaining the surgical specimens, they were cut off with a scalpel to distinguish the para-tumor and tumor tissues, then placed in separate glass vials. The collected samples were immediately transferred with ice packs, stored at –20 °C and subsequently shipped to Shanghai Weipu Testing Technology Group Co., Ltd., China.

Sample treatment for MPs analysis by LDIR and SEM

To analyse particle counts, size, and morphology of MPs, laser direct infrared (LDIR) imaging spectrometer and scanning electron microscopy (SEM) were performed. As described before,[21] the samples were placed in a beaker, concentrated nitric acid (GR 68%, Shanghai Hushi Laboratorial Equipment Co., Ltd., China, acid-to-sample ratio was 3:1) was added and incubated for 16 h at room temperature, then the beaker was placed in a graphite heating plate for 3 h to eliminate the protein. All the solvents were filtered through polytetrafluoroethylene membranes (0.45 μm pore size). All the glassware was rinsed with ethanol for 3 times and dried. Samples were weighed and recorded, then were picked up with metal tweezers, rinsed with 15 ml anhydrous ethanol and 15 ml analytical grade Milli-Q® water, vacuum filtered by using a steel membrane (13 μm pore size). After rinsing with Milli-Q® water and ethanol for 3 times, the filter membrane was immersed in ethanol solution for ultrasonication (40 kHz, 30 min), thus the particles on the filter membrane were dispersed in the ethanol solution. The membrane was removed and washed with ethanol for 3 times, then 10 ml ethanol solution was concentrated in an infrared rapid drying oven (Model: WA70-1, Hangzhou Qiwei Instrument, Co., Ltd., China) to a final volume of 150 μl and added to a high reflective glass (Low-e Microscope Slides, Kevley Technologies). LDIR test was carried out after the ethanol was completely evaporated. The Agilent 8700 LDIR spectrometer (Agilent Technologies, China) with particle analysis mode was used to obtain the counts and size distribution of MPs.[22,23] To identify the polymer types, samples were subjected to automated detection and compared with a microplastics spectra library supplied by Agilent (Microplastic Starter 1.0_1_1_1_1_2, Agilent Technologies, China).[24] The scanning wavelength ranges and spectral resolution were 1 cm^{-1} and 975–1800 cm^{-1}, respectively. Particles with 20–500 μm size and matching degree greater than 0.65 were regarded as positive detected.[25]

We applied Low-e Microscope Slides to improve the conductivity and reflectivity of LDIR. The slides were placed into the Thermo Scientific Apreo 2C for particle point localization and two-dimensional morphology shooting. Then, under the SEM, the particle points on the slides can be manually localized their position.

Sample processing procedures for MPs analysis by using Py–GC/MS

The procedure for analysing MPs by using Py–GC/MS is referred to a previous study.[7] The prostate samples were put into a beaker (100 ml) to measure the wet weight (WW), baked in an oven (60 °C) until they reached a consistent weight, then ethanol was added. The beaker was heated (60 °C, 30 min) and the ethanol was discarded. Then, trichloromethane solvent (10 g) was added, sonicated (40 kHz, 10 min for 3 times), and transferred into a new beaker, 10 g hexafluoroisopropanol solvent was added and sonicated (40 kHz, 10 min). Finally, the samples were mixed with 10 g xylene solvent, and heated at 150 °C for 10 min. The extracted liquid was condensed at 80 °C. To generate the quantitative curve, standard polymers with 0.01 g/ml concentration were prepared and tested using Py–GC/MS.

Analysis of MPs by Py–GC/MS

The sample mentioned above was subjected to pyrolysis at 550 °C by using a Frontier Lab EGA/PY-3030D instrument (Fukushima, Japan) equipped with an AS-1020E autosampler. To find any potential MPs, the resulting pyrolysis products were directly injected into a Shimadzu GC-2030 device (Shimadzu, Japan) and separated on a TG-5SILMS column (Thermo Fisher, USA).[26] The sample was first maintained at 40 °C for 2 min, raised to 320 °C at 20 °C/min, and maintained for 14 min. Mass spectra were obtained using a Shimadzu QP2020-Plus mass spectrometer coupled to the gas chromatography. To avoid re-condensation, the interface temperature was set at 320 °C. The ionization voltage was set at 70 eV, and a mass range of 29–600 m/z was analysed at a scan speed of 3333 Hz. The Lab Solutions software 4.45 was utilized for sample identification.[27]

The 11 target polymers were polystyrene (PS), polyethylene (PE), polypropylene (PP), polyvinyl chloride

(PVC), polymethyl methacrylate (PMMA), polycarbonate (PC), polyethylene terephthalate (PET), polyamide 6 (PA6), polyamide 66 (PA66), polylactic acid (PLA), and polybutylene terephthalate (PBAT). Each polymer was identified based on its specific characteristic components and ions as listed in Fig. S1. The mass spectrometry database was maintained by the National Institute of Standards and Technology (NIST).

Quality insurance and quality control (QA/QC)

During the sampling and testing process, all researchers were equipped with nitrile gloves, cotton lab coats, and hoods. Quality control was done according to a previous study.[28] Briefly, the instrument was tested once blankly under the predetermined conditions to ensure that the peaked spectrum of the instrument was without interference from the plastic fragment ions. In order to avoid the interference of plastic signals during the pre-treatment process, all reagents and solutions were undergoing vacuum filtration three times through a polytetrafluoroethylene membrane (0.45 μm pore size). The filtered reagents and solutions were used in subsequent processes only if the background detection of MPs using Py–GC/MS was blank (Fig. S1). All glassware used in the procedure was rinsed three times with filtered anhydrous ethanol before use. Furthermore, for Py–GC/MS, comprehensive quality control was performed by managing background contamination, conducting a spiking recovery experiment, and establishing limits of detection and quantification.

Statistical analysis

We used descriptive statistics to analyse the demographic characteristics of participants. Continuous and categorical variables were expressed as means ± SD, numbers and frequencies (%), respectively. The other data were expressed as means ± standard error of the mean. All statistical analyses were performed with SPSS 25.0 (IBM, Armonk, NY, USA) or GraphPad Prism 9.0 (GraphPad Software Inc., San Diego, CA, USA). Paired *t*-tests were used to compare the difference between two groups. *Pearson* correlation analysis was utilized to evaluate the correlation of MPs abundance and clinical characteristics. The definition of correlated degree was as follows: basically irrelevant: less than 0.3, weakly correlated: 0.3 to 0.5, strongly correlated: 0.5 to 0.7. The significant differences between groups were represented as $*p < 0.05$, $**p < 0.01$, and $***p < 0.001$.

Role of funders

Funding sources have no role in research design, data collection, data analysis, interpretation, or report writing.

Results

Demographic and clinical characteristics of patients

The demographic characteristics of the patients were as follows (Table 1 and Table S1): The median age, BMI, prostate volume, and PSA for the 22 patients were 66.8 years, 25.4 kg/cm^2, 45.9 ml, and 18.8 ng/ml, respectively. 14 (63.6%) patients have a Gleason score >3 + 4. The postoperative diagnosis stage of all patients was above PT2b. Of note, 11 (50%) patients had a history of smoking, while 8 (36.4%) had a history of drinking, almost all patients consumed bottled water (86.4%, 19 of 22) or take-out food (77.3%, 17 of 22).

Characteristics	Categories	Values
Age (years), Mean ± SD.	NA	66.8 ± 7.2
BMI (kg/cm^2), Mean ± SD.	NA	25.4 ± 2.6
PV (ml)	NA	45.9 ± 23.6
PSA (ng/ml)	NA	18.8 ± 13.7
Gleason score, n (%)	3 + 3	1 (4.6)
	3 + 4	7 (31.8)
	4 + 3	9 (40.9)
	4 + 4	3 (13.6)
	5 + 4	2 (9.1)
PDS, n (%)	PT2b	2 (9.1)
	PT2c	12 (54.6)
	PT3a	2 (9.1)
	PT3b	6 (27.3)
Smoking status, n (%)	Yes	11 (50.0)
	No	11 (50.0)
Drinking status, n (%)	Yes	8 (36.4)
	No	14 (63.6)
FDBW, n (%)	Never	3 (13.6)
	1–3 days/week	10 (45.5)
	≥4 days/week	9 (40.9)
FTOC, n (%)	Never	5 (22.7)
	1–3 days/week	8 (36.4)
	≥4 days/week	9 (40.9)

BMI: body mass index; PV: prostatic volume; PSA: prostate specific antigen; PDS: pathological diagnosis stage; FDBW: frequency of drinking bottled water; FTOC: frequency of take-out food consumption.

Table 1: **The demographic characteristics and clinical features of 22 patients.**

Detection and characterization of MPs in para-tumor and tumor tissues of human prostate by LDIR and SEM

We utilized LDIR to identify MPs in both para-tumor and tumor tissues of prostate. MPs such as PA, PET, PVC, and PP, along with non-MPs particles including chitin, calcium stearate, and silica were detected in para-tumor tissues (Fig. 1a and b, Fig. S2a). Similarly, MPs such as PA, PVC, PE, PET, and PS, as well as non-MPs particles including chitin, silica, and calcium stearate were detected in tumor tissues (Fig. 1c–d, Fig. S2b). Although various particles were detected, the majority of particles in the para-tumor and tumor tissues of prostate were less than 200 μm diameters (Fig. 1a–d, Fig. S3), whereas, the diameters of microplastics particles mainly ranged between 20 and 100 μm (Fig. 1e). Specifically, the distribution of microplastics particles was similar

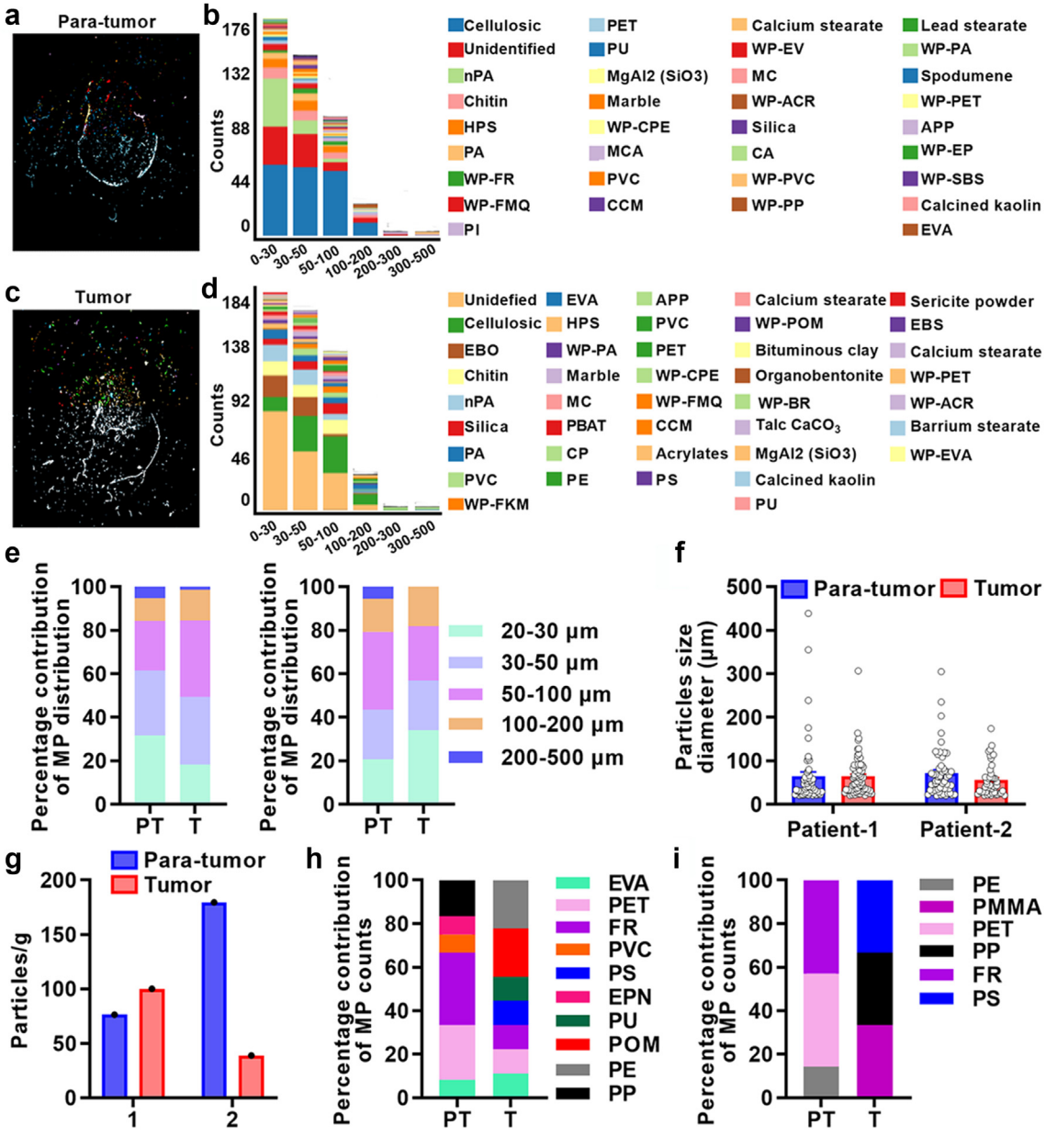

Fig. 1: **Particle size and polymer types of microplastics detected in 2 paired human prostate samples using LDIR**. (a–d) Qualitative statistical findings for MPs and non- MPs of para-tumor (a, b) and tumor tissues (c, d) using LDIR scanning with a quality match above 0.65. (e–f) Distribution of MPs in para-tumor and tumor using LDIR scanning with a quality match above 0.65. (g–i) Assessment of differences in the abundance (g) and types of MPs (h, i) in para-tumor and tumor of patient 1 and 2. PT: para-tumor, T: tumor. Abbreviations: nPA: Natural Polyamide; HPS: Hydroxypropyl starch; PA: Polyamide; WP-FR: WP-Fluororubber; WP-FMQ: WP-Fluorosilicone rubber; PI: Polyisoprene Chlorinated; PET: Polyethylene Terephthalate; PU: Polyurethane; WP-CPE: WP-Chlorinated polyethylene; MCA: Melaminecyanurate; PVC: Polyvinylchloride; CCM: Cellulose chemically modified; WP-EV: WP-Ethylene vinyl acetate copolymer; MC: Methyl cellulose; WP-ACR: WP-Acrylate copolymer; CA: Cellulose Acetate; WP-PVC: WP-Polyvinyl chloride resin; WP-PP: WP-Polypropylene; WP-PA: WP-Polyamide; WP-PET: WP-Polyethylene terephthalate; APP: Ammonium polyphosphate; WP-EP: WP-Phenolic epoxy resin; WP-SBS: WP-Styrene-butadiene-styrene; EVA: Ethylene vinyl acetate; EBO: ethylene bis oleamide; WP-FKM: WP-Fluororubber; PBAT: Poly (butyleneadipate-co-terephthalate); CP: Polyisoprene Chlorinated; PE: Polyethylene; PS: Polystyrene; WP-POM: WP-Polyoxymethylene; WP-BR: WP-Butadiene rubber; EBS: N,N′-Ethylenebis; EPN: Ethylene Propylene Norbornene; PMMA: Polymethylmethacrylate.

among 20–30 μm, 30–50 μm and 50–100 μm in para-tumor and tumor tissues of patient 1 and 2 (Fig. 1e). Additionally, MPs particle size diameter also showed no difference in these tissues (patient 1: para-tumor 64.69 ± 76.21 μm, tumor 64.78 ± 45.21 μm, patient 2: para-tumor 71.63 ± 56.12 μm, tumor 56.19 ± 37.64 μm, Fig. 1f). We then evaluated the abundance and types of MPs in these paired para-tumor and tumor tissues (Tables S2–S5, Fig. 1g–i). The abundance of MPs was 76.4, 100, 179.5 and 39.0 particles/g for para-tumor and tumor tissues of patient 1 or patient 2, respectively (Fig. 1g). Intriguingly, the types and percentage contribution of MPs particles in para-tumor and tumor tissues were different. PS was only detected in tumor tissues and the percentage of FR particles was lower in tumor tissues (Fig. 1h and i). Overall, these data demonstrate that MPs are present in both para-tumor and tumor samples from human prostate.

Subsequently, we integrated SEM with LDIR to characterize the morphological features of MPs in these tissues. Our results showed that PS was exclusively present in tumor tissues (Fig. 2a), while PP, PE, PVC and fluororubber were detected in both para-tumor and tumor tissues (Fig. 2b–e), exhibiting diverse morphologies such as particles, fibres, irregular shapes, as well as varying degrees of folding and fracturing (Fig. 2b–e).

Quantification of MPs in human prostate para-tumor and tumor tissues by Py–GC/MS

To further quantify the concentration of MPs in human prostate para-tumor and tumor tissues, we utilized Py–GC/MS to detect 11 target MPs. The spectrograms depicting characteristic components and ions for some typical MPs including PS, PE, PP, polymethyl methacrylate (PMMA), PVC, and polyethylene terephthalate (PET) from a paired set of para-tumor and tumor tissues were presented in Fig. 3 (based on specific characteristic components and ions shown in Fig. S1). We successfully identified the presence of PS, PP, PE, and PVC across all 20 paired tissue samples; their abundance is illustrated in Fig. 4a and Table S6. Interestingly, our analysis revealed significantly higher levels of PS, PE, and PVC (p = 0.0007, 0.0009 and 0.0004, paired t-tests) but not PP in tumor compared to para-tumor tissues (Fig. 4b). Given that PS, PE, and PVC was detected in nearly all samples, while PP was only found in approximately half of these samples, the comparison of PP abundance between paired tissues did not show a significant difference (Fig. 4c–f). Consistent with these observations, the abundances of PS, PP, PE and PVC were significantly elevated in tumor tissues compared to their respective para-tumor tissues in 17, 9, 17 and 17 samples, respectively (Fig. 4g–j). Together, these data indicate that PS, PP, PVC, and PE are present in para-tumor and tumor samples from human prostate. Moreover, the abundance of PS, PE, and PVC is increased in tumor tissues of human prostate.

The correlations between MPs, demographic and clinical characteristics of patients

To gain a deeper understanding of the associations between MPs and patient characteristics, we categorized the patients into different subgroups based on their lifestyle and clinical features. We examined whether there were variations in MPs abundance in para-tumor and tumor tissues among these subgroup patients. Intriguingly, we observed that an increased abundance of PP in both para-tumor and tumor tissues of patients with PSA≥10 ng/ml (p = 0.044 and 0.027, paired t-tests, Table S7). Additionally, PE abundance was elevated in tumor tissues of patients with Gleason score≤3 + 4 (p = 0.041, paired t-tests, Table S7). Moreover, PS abundance was higher in para-tumor tissues of patients who reported consuming take-out food more than 3 days per week (p = 0.003, paired t-tests, Table S8). Otherwise, no significant difference was found in MPs abundance between para-tumor and tumor tissues, among other subgroup (Tables S7 and S8).

To strengthen the clinical relevance of our findings, we further investigated the correlations between different MPs and demographic/clinical characteristics of the patients. As anticipated, a positive correlation was observed between PS abundance and frequency of take-out food consumption, furthermore, a negative correlation was found between PE abundance and Gleason score in prostate tumor tissues (r = 0.684, p < 0.001; r = –0.460, p < 0.05, pearson's correlation analysis, Fig. 5). Taken together, these data show distinct presence patterns of MPs within human prostate's para-tumor and tumor tissues.

Discussion

To the best of our knowledge, this study provides compelling evidence regarding the different abundance of MPs in para-tumor and tumor tissues of human prostate. These MPs, primarily consist of PS, PP, PE, and PVC, with diameters ranging from 20 to 50 μm. Of note, the abundance of PS, PE, and PVC except for PP was higher in tumor tissues of human prostate. Additionally, we unveiled potential correlations between MPs abundance, and demographic/clinical characteristics of 20 patients including a significant association with frequency of take-out food consumption.

Numerous studies have demonstrated the presence of MPs in human bodies using techniques such as Raman and Fourier Transform Infrared (FTIR) spectroscopy. However, these methods have limitations including weak signals, fluorescence interferences, dependence on material properties (colour, biofouling, and degradation), as well as low efficiency.[29,30] To overcome these limitations, we employed a fully automated infrared chemical imaging method called LDIR that utilized quantum cascade laser technology to identify MPs with a size range of 20–500 μm, this approach

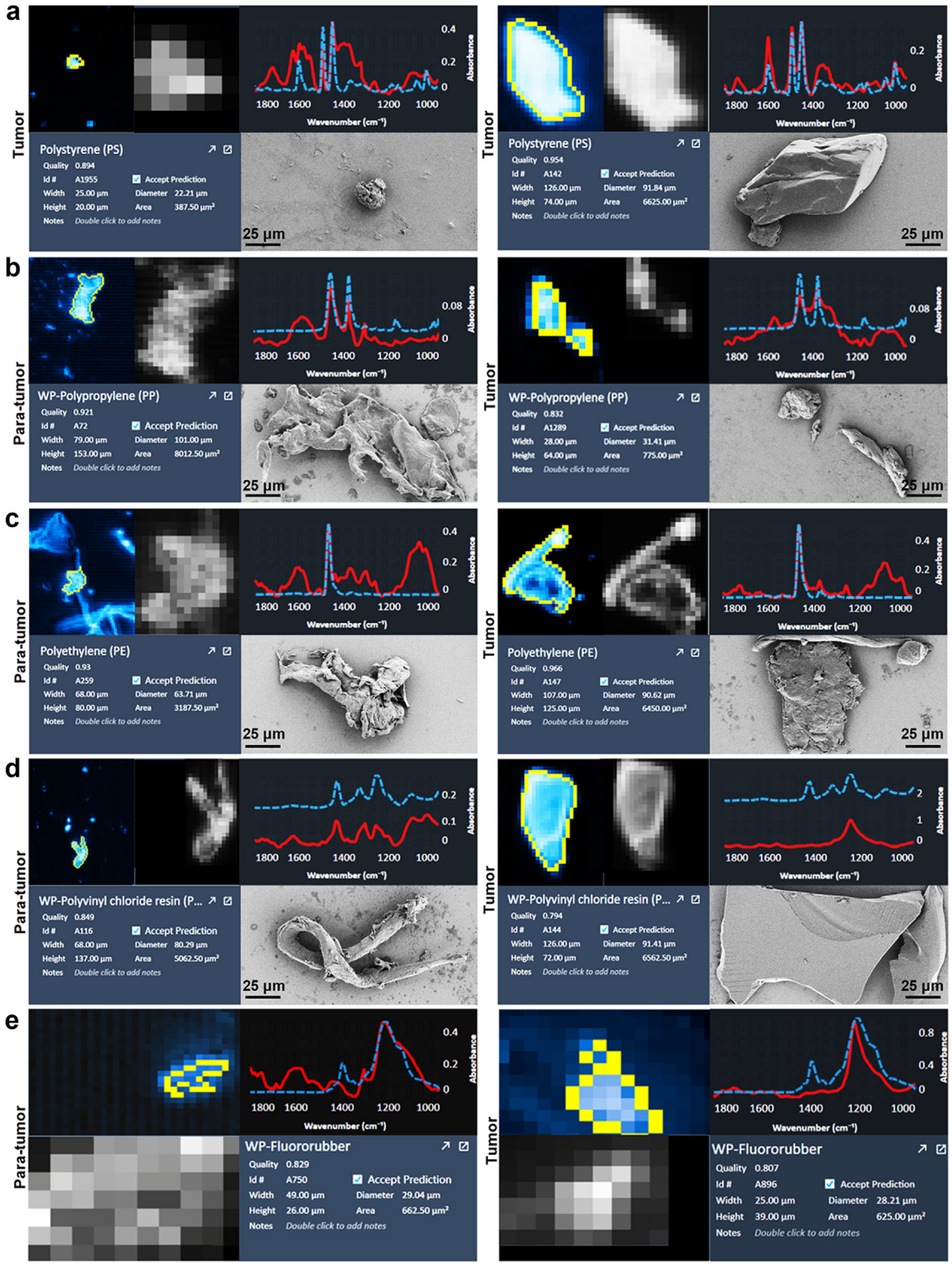

web 4C/FPO

Fig. 2: **Representative LDIR and SEM images of MPs in para-tumor and tumor tissues of human prostate**. PS was only detected in tumor tissues (a), but PP (b), PE (c), PVC (d) and fluororubber (e) was occurred in both para-tumor and tumor tissues. The representative LDIR images were the particles with highest quality. PS: Polystyrene; PE: Polyethylene; PP: Polypropylene; PVC: Polyvinylchloride.

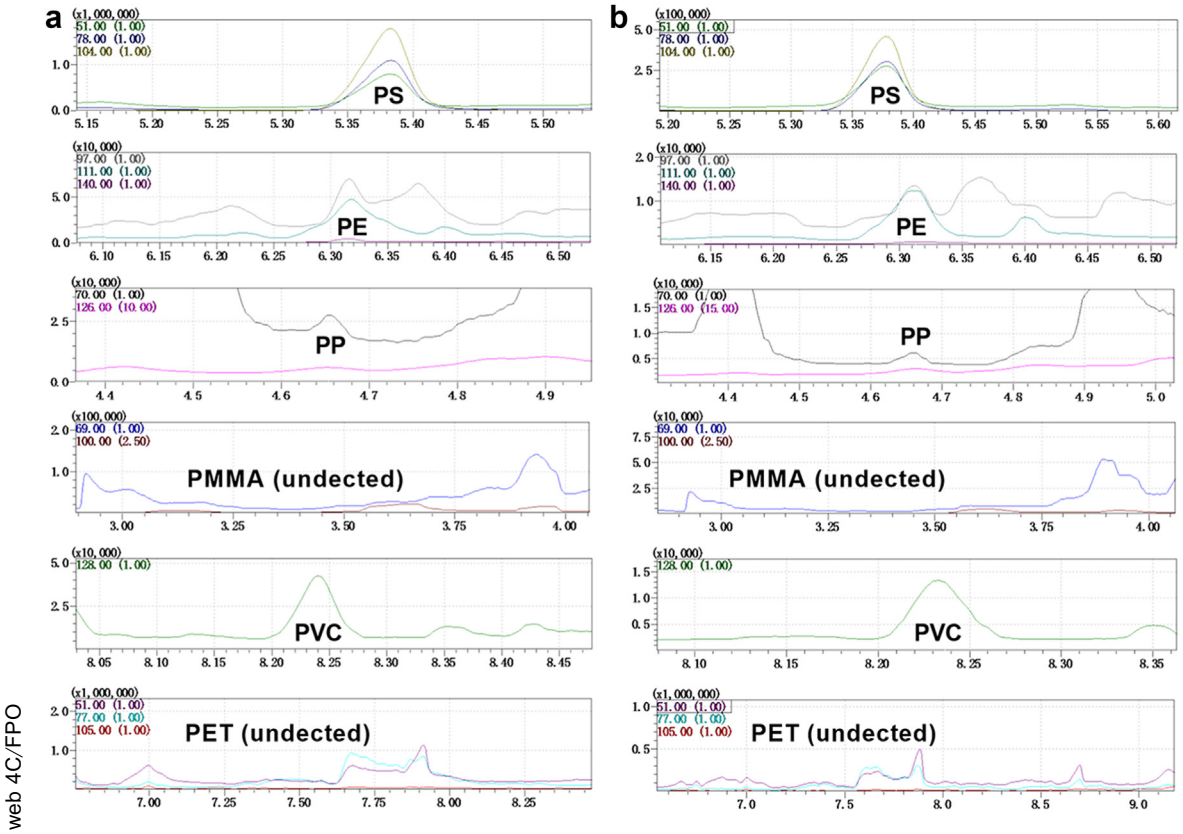

Fig. 3: **Py-GC/MS spectra of para-tumor and tumor tissues of human prostate**. Para-tumor (a) and tumor (b). PS: polystyrene; PE: polyethylene; PP: polypropylene; PMMA: polymethyl methacrylate; PVC: polyvinyl chloride; PET: polyethylene terephthalate.

improves the analytical efficiency and detection accuracy of MPs.[31] Using LDIR analysis, we discovered the presence of various types of MPs including PA, PET, PVC, and PP in both para-tumor and tumor tissues of human prostate. Interestingly, PS was only detected in the tumor tissues specifically. Furthermore, to thoroughly quantify the distribution and concentration of 11 target MPs across our sample set consisting of 20 paired human prostate samples with varying sizes ranging from 20 to 50 μm predominantly, we utilized Py–GC/MS technique which involves rapid heating to generate volatile small molecule cleavage products followed by GC and MS separation for accurate quantification.[32] MPs with a smaller diameter possess the potential to enter into the circulation and diffuse throughout the body, as evidenced by the permeation of polystyrene particles with diameters of 50 nm, 80 nm, and 240 nm into human placenta.[33] However, it remains unclear which types MPs can enter the human body through what route.

The presence of microplastics is pervasive in drinking water, food packaging materials, air, and various household products, thus our exposure to them is abundant.[34] In MPs, PS, PE, PP, and PVC are commonly used to make foam boxes and plastic cutlery, thus, they are the primary source of microplastics for people who have a history of takeout food consumption and bottled water drinking.[35–37] Usually, heat, chemical reactions as well as wear and tear on packaging all could result in the release of these microplastics.[38] MPs was widely distributed in the genitourinary system. Firstly, the distribution of MPs in urine was PET (50%), PS (36%), PE (23%) and PMMA (5%).[39] Then, the primary MPs found in testicular tissue and normal human semen are PS, PP, PE, PET, PVC, PC, and polyoxymethylene (POM).[11,40] These results suggest that MPs may also present in the prostate gland. We found that the mean abundance of total MPs in tumor tissues (290.3 μg/g) was much higher than para-tumor (181.0 μg/g) of human prostate samples. Intriguingly, the abundance of PS, PE, and PVC, but not PP, was increased in tumor tissues, and PP was only detected in about 50% para-tumor and tumor tissues of human prostate samples. A recent study also found the aggregation of MPs in human prostate, they identified 4 different types of plastic, and the most common MPs were polyamide.[41] Together, these findings suggest that MPs may accumulate in the prostate and that these MPs might correlate with prostate cancer.

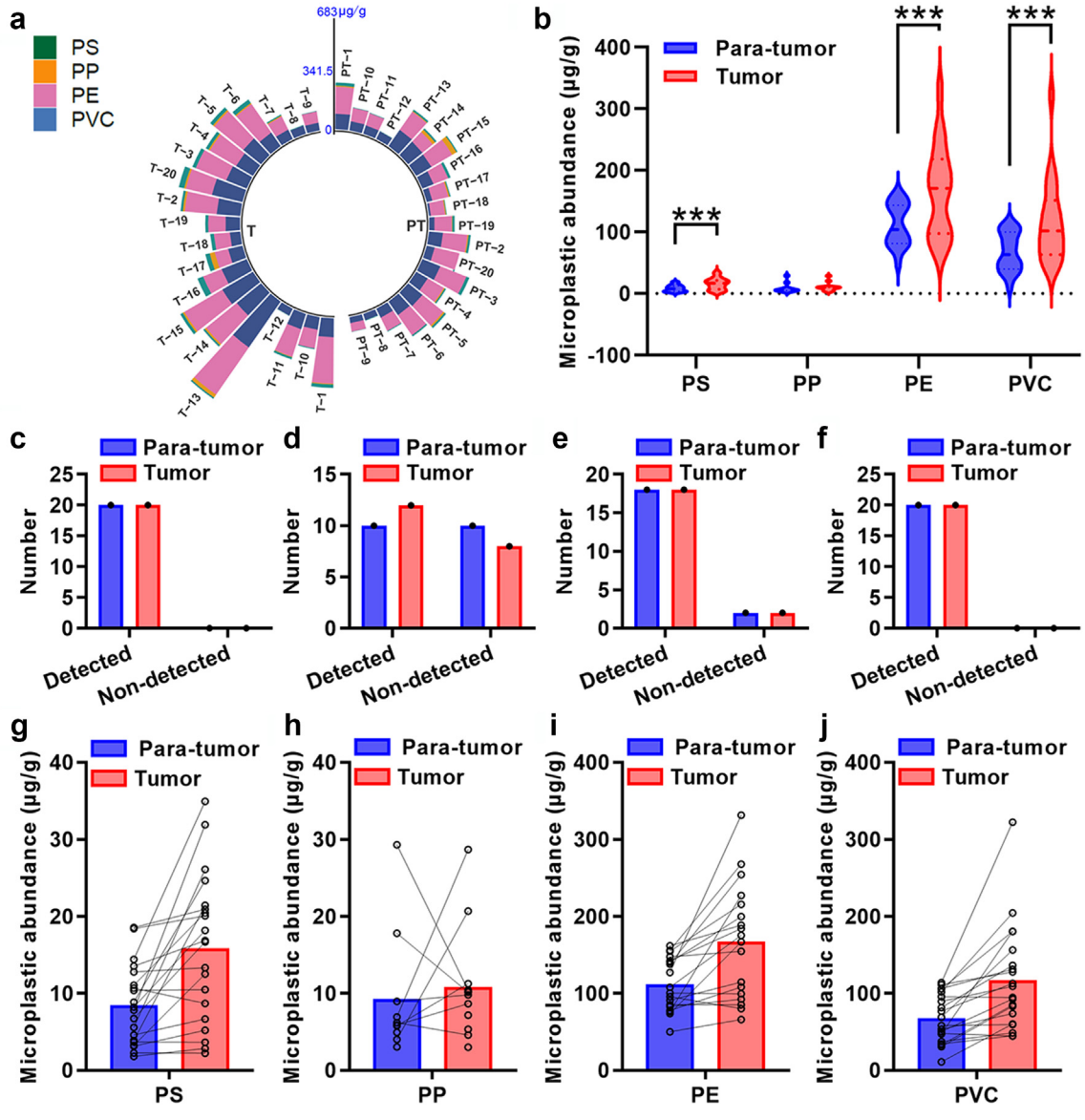

web 4C/FPO

Fig. 4: **Abundance of MPs in para-tumor and tumor tissues of human prostate using Py-GC/MS**. (a) Concentrations of MPs in individual paired para-tumor and tumor tissues. (b) The abundance of PS, PP, PE and PVC in these 20 paired tissues. (c–f) Detection of PS (c), PP (d), PE (e), and PVC (f) in the tissues. (g–j) Detailed abundance of PS (g), PP (h), PE (i), and PVC (j) in each paired para-tumor and tumor tissue. PT: para-tumor and T: tumor. ***$p < 0.001$ and data are analysed by paired t test. PS: polystyrene; PP: polypropylene; PE: polyethylene; PVC: polyvinyl chloride.

The underlying mechanisms and processes responsible for the presence of MPs in human tumor systems is still unknown. MPs were intake into human body accompany with plastic product. Majority of MPs exhibit strong resistance to acidic environments; thus, the surface and morphology of MPs were not altered after they passed through the colon.[42] Intestinal epithelial cells are more likely to endocytose tiny particles (<150 μm) and release them into the circulation system.[43] Furthermore, MPs have the ability to translocate into lymphoid tissues after being phagocytosis by macrophages, bypassing the main intestinal clearance pathway and reaching the bloodstream,[44] then accumulate in human bodies. MPs may also enter the genitourinary system since they have been detected in human semen, testicular and prostate samples.[11,40,41] MPs exposure results in an increase in ROS levels, activation of the p38 and MAPK signalling pathways,[45] thus may result in male urinary tumor system damage. Besides, toxic organic compounds, such as phthalates, BPA, and Polychlorinated biphenyls (PCBs),

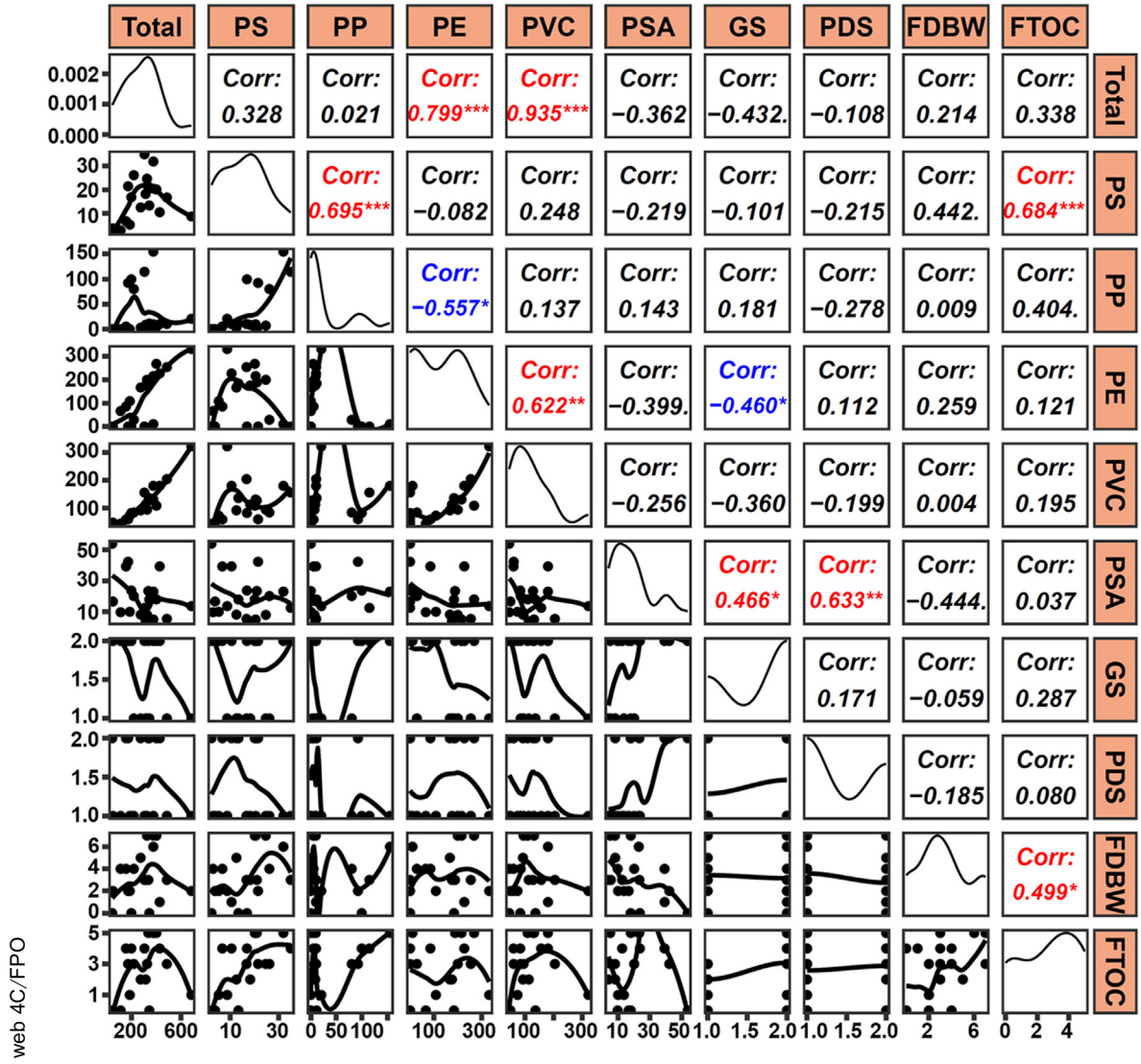

Fig. 5: **Relationships between MPs concentrations and clinical characteristics of patients**. Diagonal plots illustrate the distribution of data in logarithmic ratios. Lower plots display the scatter plots of data, while the upper plots indicate the correlation coefficients (r). Significant correlations are highlighted in red or blue. *$p < 0.05$; **$p < 0.01$; ***$p < 0.001$ and data are analysed by *Pearson's* correlation analysis. PS: polystyrene; PP: polypropylene; PE: polyethylene; PVC: polyvinyl chloride. PSA: prostate specific antigen; GS: Gleason score; PDS: pathological diagnosis stage; FDBW: frequency of drinking bottled water; FTOC: frequency of take-out food consumption.

also could adsorb onto MPs and enter the organism, thus exerting toxic effects on the male reproductive system.[46–48] Considering the different pattern of MPs in tumor and para-tumor tissues of human prostate, the cell proliferation, migration, and inflammatory responses of tumor tissues may affect the accumulation of MPs.[49]

Further, relationship between MPs and human health is still unclear. The higher detective ratio and concentration of MPs in cirrhotic liver tissue,[50] increased MPs concentration of faecal in patients with inflammatory bowel disease, as well as detection of acrylic, PET, and phenoxy resins in tumor tissue of human lung,[51,52] suggest the potential relationship of MPs and human disease. As for the animal model, there were increased levels of inflammation and apoptotic prostate epithelial cells in the prostates of mice treated with high-fat diet and low doses of MPs.[53] Polystyrene microplastics exposure also results in augmented oxidative stress, imbalance of blood hormone levels, and declined fertility of male mice.[54] Together with our data, the accumulation of MPs may have some relationship with prostate cancer, but there is a need to enhance the representativeness of the study and the reliability of the

conclusions by expanding the sample size and usage of more diverse sample sources in the future studies.

Our study also has some limitations. Firstly, we did not detect the presence of MPs in the healthy prostate. Due to the exploratory nature of the study, we were unable to perform formal sample size calculations. The sample size of our study is not so big to represent the entire prostate cancer population. Further study of large sample size and complex designs is needed to explore the relationship between microplastics exposure and risk of prostate cancer. Multiple testing is also not applicable due to data limitations. Lastly, we only detected the MPs and 11 target MPs by using LDIR, SEM and Py–GC/MS, improved microplastics detection techniques should be used in the future research to give an accurate overview of MPs in human prostate samples. In this paper, only correlations between MPs and clinical features in human prostate tissue were calculated, and these results are insufficient to draw a robust relationship between MPs exposure and prostate cancer development. Despite these limitations, our study provides valuable insights into the presence of MPs in the human prostate, sheds light on the potential implications of MPs on prostate health. Future longitudinal studies should be conducted to enhance the understanding of the dynamic interplay and potential causal connections between MPs and prostate health over time.

Contributors

All the authors have read and approved the final version of the manuscript. C.D., J.Z. and Z.F. conceptualize and design the study; C.D., Y.Y. and Q.Z. conducted the study and collected the data; J.Z., Z.Z., Y.Y. and Z.F. performed experiments; Z.J. and H.J. accessed and verified the data; C.D. and J.Z. performed data analysis; C.D., Y.Y. and Z.J. drafted the manuscript; Z.F., Z.Z., Y.Y. and H.J. critically revised the manuscript.

Data sharing statement

Data are available on request from the authors.

Declaration of interests

The authors declare no competing financial interests.

Acknowledgements

This work was supported by the National Key Research and Development Program of China (2022YFC2702600) and the National Natural Science Foundation of China (Grant No. 82071698, No. 82101676 , No. 82301792 and No. 82271630). We also want to thank Shanghai Weipu Testing Technology Group Co., Ltd., for testing microplastics.

Appendix A. Supplementary data

Supplementary data related to this article can be found at https://doi.org/10.1016/j.ebiom.2024.105360.

References

1 Wang Y, Xu X, Jiang G. Microplastics exposure promotes the proliferation of skin cancer cells but inhibits the growth of normal skin cells by regulating the inflammatory process. *Ecotoxicol Environ Saf*. 2023;267:115636.
2 Osman AI, Hosny M, Eltaweil AS, et al. Microplastic sources, formation, toxicity and remediation: a review. *Environ Chem Lett*. 2023:1–41.
3 Landrigan PJ, Raps H, Cropper M, et al. The minderoo-Monaco commission on plastics and human health. *Ann Glob Health*. 2023;89(1):23.
4 Jiang B, Kauffman AE, Li L, et al. Health impacts of environmental contamination of micro- and nanoplastics: a review. *Environ Health Prev Med*. 2020;25(1):29.
5 Phuong NN, Duong TT, Le TPQ, et al. Microplastics in Asian freshwater ecosystems: current knowledge and perspectives. *Sci Total Environ*. 2022;808:151989.
6 Zuri G, Karanasiou A, Lacorte S. Microplastics: human exposure assessment through air, water, and food. *Environ Int*. 2023;179:108150.
7 Liu S, Liu X, Guo J, et al. The association between microplastics and microbiota in placentas and meconium: the first evidence in humans. *Environ Sci Technol*. 2023;57(46):17774–17785.
8 Jenner LC, Rotchell JM, Bennett RT, Cowen M, Tentzeris V, Sadofsky LR. Detection of microplastics in human lung tissue using μFTIR spectroscopy. *Sci Total Environ*. 2022;831:154907.
9 Hirt N, Body-Malapel M. Immunotoxicity and intestinal effects of nano- and microplastics: a review of the literature. *Part Fibre Toxicol*. 2020;17(1):57.
10 Leslie HA, van Velzen MJM, Brandsma SH, Vethaak AD, Garcia-Vallejo JJ, Lamoree MH. Discovery and quantification of plastic particle pollution in human blood. *Environ Int*. 2022;163:107199.
11 Zhao Q, Zhu L, Weng J, et al. Detection and characterization of microplastics in the human testis and semen. *Sci Total Environ*. 2023;877:162713.
12 Prata JC, da Costa JP, Lopes I, Duarte AC, Rocha-Santos T. Environmental exposure to microplastics: an overview on possible human health effects. *Sci Total Environ*. 2020;702:134455.
13 An R, Liu J, Chu X, et al. Polyamide 6 microplastics as carriers led to changes in the fate of bisphenol A and dibutyl phthalate in drinking water distribution systems: the role of adsorption and interfacial partitioning. *J Hazard Mater*. 2024;476:134997.
14 Ullah S, Ahmad S, Guo X, et al. A review of the endocrine disrupting effects of micro and nano plastic and their associated chemicals in mammals. *Front Endocrinol*. 2022;13:1084236.
15 Gandaglia G, Leni R, Bray F, et al. Epidemiology and prevention of prostate cancer. *Eur Urol Oncol*. 2021;4(6):877–892.
16 Zhu Y, Mo M, Wei Y, et al. Epidemiology and genomics of prostate cancer in Asian men. *Nat Rev Urol*. 2021;18(5):282–301.
17 Barul C, Parent ME. Occupational exposure to polycyclic aromatic hydrocarbons and risk of prostate cancer. *Environ Health*. 2021;20(1):71.
18 Kumar R, Manna C, Padha S, et al. Micro(nano)plastics pollution and human health: how plastics can induce carcinogenesis to humans? *Chemosphere*. 2022;298:134267.
19 Zhao T, Shen L, Ye X, et al. Prenatal and postnatal exposure to polystyrene microplastics induces testis developmental disorder and affects male fertility in mice. *J Hazard Mater*. 2023;445:130544.
20 Song JH, Hwang B, Kim SB, Choi YH, Kim WJ, Moon SK. Bisphenol A modulates proliferation, apoptosis, and wound healing process of normal prostate cells: involvement of G2/M-phase cell cycle arrest, MAPK signaling, and transcription factor-mediated MMP regulation. *Ecotoxicol Environ Saf*. 2023;249:114358.
21 Ourgaud M, Phuong NN, Papillon L, et al. Identification and quantification of microplastics in the marine environment using the laser direct infrared (LDIR) technique. *Environ Sci Technol*. 2022;56(14):9999–10009.
22 Huang S, Huang X, Bi R, et al. Detection and analysis of microplastics in human sputum. *Environ Sci Technol*. 2022;56(4):2476–2486.
23 Xue J, Xu Z, Hu X, Lu Y, Zhao Y, Zhang H. Microplastics in maternal amniotic fluid and their associations with gestational age. *Sci Total Environ*. 2024;920:171044.
24 Song X, Chen T, Chen Z, et al. Micro(nano)plastics in human urine: a surprising contrast between Chongqing's urban and rural regions. *Sci Total Environ*. 2024;917:170455.
25 Deng L, Xi H, Wan C, Fu L, Wang Y, Wu C. Is the petrochemical industry an overlooked critical source of environmental microplastics? *J Hazard Mater*. 2023;451:131199.
26 Ke D, Zheng J, Liu X, et al. Occurrence of microplastics and disturbance of gut microbiota: a pilot study of preschool children in Xiamen, China. *eBioMedicine*. 2023;97:104828.
27 Wang T, Yi Z, Liu X, et al. Multimodal detection and analysis of microplastics in human thrombi from multiple anatomically distinct sites. *eBioMedicine*. 2024;103:105118.

28 Kutralam-Muniasamy G, Shruti VC, Pérez-Guevara F, Roy PD, Elizalde-Martínez I. Common laboratory reagents: are they a double-edged sword in microplastics research? *Sci Total Environ*. 2023;875:162610.
29 Elert AM, Becker R, Duemichen E, et al. Comparison of different methods for MP detection: what can we learn from them, and why asking the right question before measurements matters? *Environ Pollut*. 2017;231(Pt 2):1256–1264.
30 Araujo CF, Nolasco MM, Ribeiro AMP, Ribeiro-Claro PJA. Identification of microplastics using Raman spectroscopy: latest developments and future prospects. *Water Res*. 2018;142:426–440.
31 Tian X, Beén F, Bäuerlein PS. Quantum cascade laser imaging (LDIR) and machine learning for the identification of environmentally exposed microplastics and polymers. *Environ Res*. 2022;212(Pt D):113569.
32 Seeley ME, Lynch JM. Previous successes and untapped potential of pyrolysis-GC/MS for the analysis of plastic pollution. *Anal Bioanal Chem*. 2023;415(15):2873–2890.
33 Wick P, Malek A, Manser P, et al. Barrier capacity of human placenta for nanosized materials. *Environ Health Perspect*. 2010;118(3):432–436.
34 Vethaak AD, Legler J. Microplastics and human health. *Science*. 2021;371(6530):672–674.
35 Koelmans AA, Mohamed Nor NH, Hermsen E, Kooi M, Mintenig SM, De France J. Microplastics in freshwaters and drinking water: critical review and assessment of data quality. *Water Res*. 2019;155:410–422.
36 Bai CL, Liu LY, Guo JL, Zeng LX, Guo Y. Microplastics in take-out food: are we over taking it? *Environ Res*. 2022;215(Pt 3):114390.
37 Shruti VC, Kutralam-Muniasamy G. Migration testing of microplastics in plastic food-contact materials: release, characterization, pollution level, and influencing factors. *TrAC, Trends Anal Chem*. 2024;170:117421.
38 Du F, Cai H, Zhang Q, Chen Q, Shi H. Microplastics in take-out food containers. *J Hazard Mater*. 2020;399:122969.
39 Pironti C, Notarstefano V, Ricciardi M, Motta O, Giorgini E, Montano L. First evidence of microplastics in human urine, a preliminary study of intake in the human body. *Toxics*. 2022;11(1).
40 Montano L, Giorgini E, Notarstefano V, et al. Raman Microspectroscopy evidence of microplastics in human semen. *Sci Total Environ*. 2023;901:165922.
41 Demirelli E, Tepe Y, Oğuz U, et al. The first reported values of microplastics in prostate. *BMC Urol*. 2024;24(1):106.
42 Stock V, Fahrenson C, Thuenemann A, et al. Impact of artificial digestion on the sizes and shapes of microplastic particles. *Food Chem Toxicol*. 2020;135:111010.
43 Fournier E, Leveque M, Ruiz P, et al. Microplastics: what happens in the human digestive tract? First evidences in adults using in vitro gut models. *J Hazard Mater*. 2023;442:130010.
44 Wu B, Wu X, Liu S, Wang Z, Chen L. Size-dependent effects of polystyrene microplastics on cytotoxicity and efflux pump inhibition in human Caco-2 cells. *Chemosphere*. 2019;221:333–341.
45 Xie X, Deng T, Duan J, Xie J, Yuan J, Chen M. Exposure to polystyrene microplastics causes reproductive toxicity through oxidative stress and activation of the p38 MAPK signaling pathway. *Ecotoxicol Environ Saf*. 2020;190:110133.
46 Mínguez-Alarcón L, Hauser R, Gaskins AJ. Effects of bisphenol A on male and couple reproductive health: a review. *Fertil Steril*. 2016;106(4):864–870.
47 Deng Y, Yan Z, Shen R, Huang Y, Ren H, Zhang Y. Enhanced reproductive toxicities induced by phthalates contaminated microplastics in male mice (Mus musculus). *J Hazard Mater*. 2021;406:124644.
48 Williams RS, Curnick DJ, Brownlow A, et al. Polychlorinated biphenyls are associated with reduced testes weights in harbour porpoises (Phocoena phocoena). *Environ Int*. 2021;150:106303.
49 Brynzak-Schreiber E, Schögl E, Bapp C, et al. Microplastics role in cell migration and distribution during cancer cell division. *Chemosphere*. 2024;353:141463.
50 Horvatits T, Tamminga M, Liu B, et al. Microplastics detected in cirrhotic liver tissue. *eBioMedicine*. 2022;82:104147.
51 Li Y, Shi T, Li X, et al. Inhaled tire-wear microplastic particles induced pulmonary fibrotic injury via epithelial cytoskeleton rearrangement. *Environ Int*. 2022;164:107257.
52 Yan Z, Liu Y, Zhang T, Zhang F, Ren H, Zhang Y. Analysis of microplastics in human feces reveals a correlation between fecal microplastics and inflammatory bowel disease status. *Environ Sci Technol*. 2022;56(1):414–421.
53 Gao D, Zhang C, Guo H, et al. Low-dose polystyrene microplastics exposure impairs fertility in male mice with high-fat diet-induced obesity by affecting prostate function. *Environ Pollut*. 2024;346:123567.
54 Wei Z, Wang Y, Wang S, Xie J, Han Q, Chen M. Comparing the effects of polystyrene microplastics exposure on reproduction and fertility in male and female mice. *Toxicology*. 2022;465:153059.